

Low temperature vortex phase diagram of Bi₂Sr₂CaCu₂O₈: a magnetic penetration depth study.

R. Prozorov^a, R. W. Giannetta^a, T. Tamegai^b, P. Guptasarma^c, and D.G. Hinks^c

^a Loomis Laboratory of Physics, University of Illinois at Urbana-Champaign, 1110 West Green St, Urbana, Illinois 61801.

^b Department of Applied Physics, The University of Tokyo, Hongo, Bunkyo-ku, Tokyo, 113-8656, Japan.

^c Chemistry and Materials Science Division, Argonne National Laboratory, Argonne, Illinois 60439

We report measurements of the magnetic penetration depth $\lambda_m(T)$ in the presence of a DC magnetic field in optimally doped *BSCCO-2212* single crystals. Warming, after magnetic field is applied to a zero-field cooled sample, results in a non-monotonic $\lambda_m(T)$, which does not coincide with a curve obtained upon field cooling, thus exhibiting a hysteretic behaviour. We discuss the possible relation of our results to the vortex decoupling, unbinding, and dimensional crossover.

1. INTRODUCTION

The field-temperature phase diagram of Bi-2212 is well studied at high and intermediate temperatures [1-5]. At low temperatures, the situation is less clear. Below $t=T/T_c \sim 0.2$ the fishtail disappears, persistent current density increases almost exponentially (Fig.1), and the relaxation rate changes [2]. Theory predicts various peculiarities in vortex behavior at low temperatures, such as dimensional crossover in the pinning mechanism [2], topological transition in the vortex lattice [3,4], electromagnetic decoupling and a related Kosterlitz-Thouless type transition [5].

We present new experimental results on $\lambda_m(T)$ at low temperatures and discuss their relevance to the aforementioned scenarios.

2. EXPERIMENTAL

Magnetic penetration depth measurements were performed using a tunnel-diode driven 11 MHz LC resonator [6] operating in a ³He refrigerator. The resonance frequency shift

$\Delta f = f(T) - f(T_{min})$ is related to $\Delta\lambda_m$ via $\Delta\lambda_m = -G\Delta f$, where G is the sample and apparatus dependent calibration constant [7]. Magnetization was measured using a *Quantum Design* SQUID.

3. RESULTS

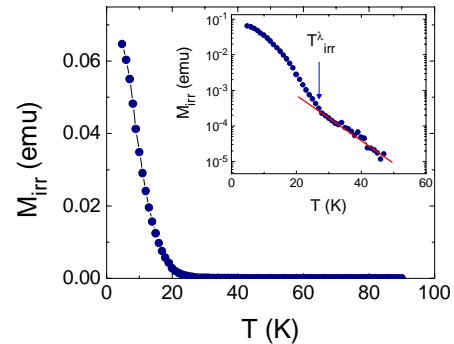


Figure 1. Irreversible part of the magnetic moment in *BSCCO* at $H=300$ G. Inset: Log plot.

Figure 1 presents the irreversible part of the magnetic moment, $M_{irr} = (M_{\downarrow} - M_{\uparrow})/2$, as a function of temperature at $H=300$ G. Here, M_{\downarrow} is the descending and M_{\uparrow} is the ascending branch of

$M(H)$ loop, respectively. The inset shows the same data in a log plot. Above certain temperature, T_{irr}^λ , $M_{irr}(T)$ is exponentially suppressed indicating a weak pinning regime.

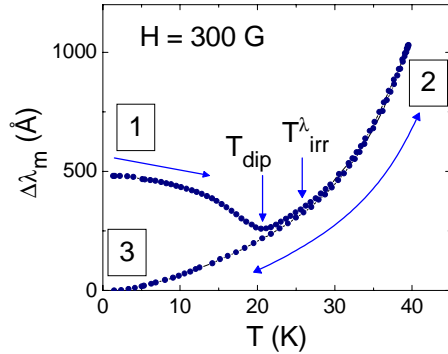


Figure 2. $\Delta\lambda_m(T)$ at $H=300$ G. Symbols and arrows are described in the text.

Figure 2 shows the magnetic penetration depth $\Delta\lambda_m(T)$ measured at $H=300$ G. The sample was cooled to $T=1$ K and magnetic field was applied (point 1 in Fig.2). The sample was then warmed up (1→2) and cooled down (2→3). Subsequent warming and cooling did not modify the temperature dependence of $\lambda_m(T)$ – it always followed the “reversible” (3→2→3) curve. There are two distinctive points: $T_{dip}(H)$ above which $\lambda_m(T)$ is dominated by the reversible (3→2) curve; and $T_{irr}^\lambda(H)$ where reversible and irreversible curves merge. The observed hysteresis in $\lambda_m(T)$ can be attributed to a crossover from a strong to a weak pinning regime, which is consistent with the measurements of the irreversible magnetization in Fig. 1.

We measured $\lambda_m(T)$ at different values of the DC magnetic field and determined both $T_{dip}(H)$ and $T_{irr}^\lambda(H)$. The resulting phase diagram is shown in Fig.3. The usual irreversibility temperature, $T_{irr}(H)$, determined from the AC susceptibility measurements is also shown for comparison.

Unlike $T_{irr}(H)$, neither $T_{dip}(H)$ nor $T_{irr}^\lambda(H)$ extrapolate to T_c , but at most to $t=0.5$. This fact favors an unbinding transition scenario, in

which the Kosterlitz - Thouless temperature sets the temperature scale [5].

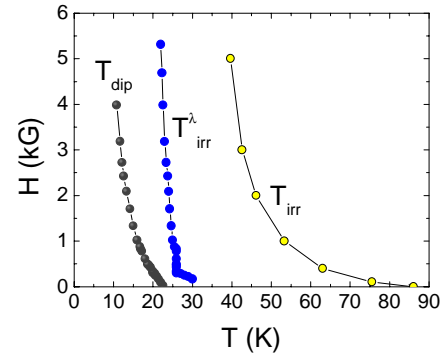


Figure 3. Low temperature phase diagram of BSCCO-2212 from the measurements of $\Delta\lambda_m$.

Alternative mechanisms could be a dimensional crossover in the pinning mechanism [2] or a topological transition in the vortex structure [3,4]. We also note that the fishtail feature exists only between T_{dip} and T_{irr} lines, Fig.3, where the pinning is weak. This would imply a collective creep, dynamic explanation of the fishtail. However, a knee in $T_{irr}^\lambda(H)$ at $H \approx 400$ G (onset of a fishtail) could be an indication of the entanglement crossover [4] in the vortex structure in this temperature region.

We thank Vadim Geshkenbein for useful discussions. This work was supported by Science and Technology Center for Superconductivity Grant No. NSF-DMR 91-20000.

REFERENCES

1. P. Kes *et al.*, J. Phys. I 6 (1996) 2327.
2. M. Nideröst *et al.*, Phys. Rev. B 53 (1996) 9286.
3. R. Šášik and D. Stroud, Phys. Rev. B 52 (1995) 3696.
4. D. Ertas and D. R. Nelson, Physica C 272 (1996) 79.
5. M. J. W. Dodgson *et al.*, cond- mat/9902244
6. C. T. Van Degriфт, Rev. Sci. Inst. 46 (1975) 599.
7. A. Carrington *et al.*, Phys. Rev. Lett. 83 (1999) 4172.